



Appendix F: Summary of Geologic Data and Development of *A Priori* Rupture Models for the Elsinore, San Jacinto, and Garlock Faults

By Timothy E. Dawson¹, Tom K. Rockwell²,
Ray J. Weldon II³, and Chris J. Wills⁴

USGS Open File Report 2007-1437F
CGS Special Report 203F
SCEC Contribution #1138F
Version 1.0

2008

U.S. Department of the Interior
U.S. Geological Survey

California Department of Conservation
California Geological Survey

¹U.S. Geological Survey, Menlo Park, California

³San Diego State University, California

³University of Oregon, Eugene

⁴California Geological Survey, Sacramento, California

U.S. Department of the Interior
DIRK KEMPTHORNE, Secretary

U.S. Geological Survey
Mark D. Myers, Director

State of California
ARNOLD SCHWARZENEGGER, Governor

The Resources Agency
MIKE CHRISMAN, Secretary for Resources

Department of Conservation
Bridgett Luther, Director

California Geological Survey
John G. Parrish, Ph.D., State Geologist

U.S. Geological Survey, Reston, Virginia 2008

For product and ordering information:
World Wide Web: <http://www.usgs.gov/pubprod>
Telephone: 1-888-ASK-USGS

For more information on the USGS—the Federal source for science about the Earth,
its natural and living resources, natural hazards, and the environment:
World Wide Web: <http://www.usgs.gov>
Telephone: 1-888-ASK-USGS

Suggested citation:
Dawson, T.E., Rockwell, T.K., Weldon, R.J., II, and Wills, C.J. 2008, Summary of
geologic data and development of *a priori* rupture models for the Elsinore, San
Jacinto, and Garlock Faults, *Appendix F in The Uniform California Earthquake
Rupture Forecast, version 2 (UCERF 2)*: U.S. Geological Survey Open-File Report
2007-1437F and California Geological Survey Special Report 203F, 23 p.
[<http://pubs.usgs.gov/of/2007/1437/f/>].

Any use of trade, product, or firm names is for descriptive purposes only and does
not imply endorsement by the U.S. Government.

Although this report is in the public domain, permission must be secured from the
individual copyright owners to reproduce any copyrighted material contained within
this report.

Contents

Introduction.....	1
Fault Sections and Segmentation.....	1
Rupture Models.....	2
Elsinore Fault.....	6
Elsinore Fault Rupture Models.....	9
San Jacinto fault.....	11
San Jacinto Fault Rupture Models.....	15
Garlock Fault.....	16
Garlock Fault Rupture Models.....	18
References.....	19

Appendix F¹

Summary of Geologic Data and Development of *A Priori* Rupture Models for the Elsinore, San Jacinto and Garlock faults

Timothy Dawson¹, Tom Rockwell², Ray Weldon³, and Chris Wills⁴

¹ U.S. Geological Survey

² San Diego State University

³ University of Oregon

⁴ California Geological Survey

Introduction

This appendix to the WGCEP Earthquake Rate Model 2 summarizes geologic data and documents the development of the rupture models for the Elsinore, San Jacinto, and Garlock faults. For the summary of available geologic data, the documentation is organized by fault and fault segment and includes a summary of slip rates, event timing and recurrence, slip-per-event, and historical seismicity for each segment. This information is compiled from the published literature as well as newer studies that have not yet been published. For the unpublished data, we either are familiar, having visited the paleoseismic sites, or participated in the data collection, or we have solicited the principal investigators at each site for their latest results. While these unpublished results are preliminary, we have chosen to include them because the results were considered in development of the rupture models and it is unlikely that the sites will be formally published before the WGCEP Earthquake Rate Model is finalized. The second part of this document describes the construction of the rupture models used in the WGCEP Earthquake Rate Model 2, and the rationale that went into the construction of these models, with a summary of what types of data were considered when the rupture models were created.

Fault Sections and Segmentation

For the purposes of this discussion, the term *fault segment* follows the convention of WG02 that considers fault segments to be "the basic building block for each fault, the shortest section considered capable of repeatedly rupturing to produce large earthquake of interest here.". This differs from the term *fault section* used elsewhere by the current Working Group on California Earthquake Probabilities. Appendix A of this report (Wills and others, 2007) uses the term *fault section* to describe parts of faults with differences in any of the parameters in the "fault section database". Fault sections can also be defined based on changes in geometry, relative age, geomorphic expression, or other geologic criteria. In this compilation, we use the sections as defined by changes in fault parameters as in Appendix A. With few exceptions, these fault sections are also considered to be fault segments. The only sections that are not also considered as potential segments are the parallel overlapping sections on opposite sides of pull-apart basins. These sections are designated mostly for accounting purposes to partition the slip rate between the parallel strands. For the purposes of generating the rupture models, we have in most cases adopted the boundaries of segments established by previous working groups, but we have proposed new sections on the southern San Andreas fault, as well as changes to the sections on the San Jacinto and Elsinore faults as described in Appendix A. The goal of this summary is to briefly describe the general characteristics of each fault segment that may influence the fault's

¹ *in*: Earthquake Rate Model 2 of the Working Group on California Earthquake Probabilities.

rupture behavior as well as provide a basis for the reader to evaluate the types of data that were considered in the construction of the rupture models for each fault. For the most part, these descriptions are a restatement of the summaries provided by WGCEP 95, Appendix C. We have supplemented these descriptions by new or reinterpreted paleoseismic data that are now available and considered in the construction of the rupture models.

Rupture Models

The goal of the segmentation-based fault models is to determine the magnitude and long-term rate of single- and multi-segment combinations on a given fault. The first step in this process is to take the fault segments and determine the rupture frequencies for each segment or combinations of segments. In order to construct A-fault rupture frequencies, the fault sections of the *Fault Section Database 2.0* were first combined into rupture segments. As described previously, fault sections are defined by changes in geometry, style, slip rate or bends and stepovers in the fault trace. Because these features are often observed to limit rupture, most fault sections in the Fault Section Database were inferred to be able to produce rupture either independently or with some number of contiguous sections. In our nomenclature, we use the term *fault segments* to refer to either fault sections or combinations of fault sections that either rupture individually or together during an earthquake. The rupture models presented here only consider full-segment ruptures. Appendix G describes an alternative approach and results for an unsegmented model for the A-faults.

All rupture segments and all multi-segment combinations are listed in the A-Fault segment table (hereafter referred to as the *A_FaultsSegmentData* or Table 1). Because the sum of the frequencies of all rupture combinations that involve a segment during a given interval of time must equal the total frequency of rupture for that segment, the recurrence intervals of each segment were compiled and converted into rupture frequencies.

Because many different combinations of single- and multiple- segment ruptures can satisfy the recurrence data, additional information or constraints are required to determine a unique combination of ruptures that satisfies the recurrence data. To span the range of possible models, it was decided to construct three categories of models: 1) A model that satisfies the recurrence data with the minimum number of ruptures, 2) A model that satisfies the data with the maximum number of ruptures, and 3) A model that was considered to be most consistent with other information, such as the extent of historic ruptures, the similarity of timing of paleoseismic ruptures on adjacent segments, the similarity of slip rate and displacement between segments, information on slip-per-event and inferred rupture extents, and the degree to which segment boundaries are likely to limit multi-segment ruptures. Because it is impossible to quantify the relative significance of these constraints, this model was designated the “geologic insight” model and was developed by consensus by a group of geologists familiar with all of the A-faults at a meeting in San Diego, CA on June 12-14, 2007 (Chaired by Ray Weldon and Ned Field; attendees included Tim Dawson, Vipin Gupta, Tom Rockwell, David Schwartz, and Chris Wills) who used the available data and expert opinion to form a model that honors the geologic data as well as their understanding of how the fault distributes ruptures along its length. These models were presented and additional input was solicited from a larger group of earth scientists at a WGCEP sponsored meeting held at the University of Southern California on November 13, 2006.

Each A-fault was considered in turn and all of the available data on recurrence intervals, timing and extent of historic and prehistoric earthquakes, and slips-per-event data were compiled and discussed. This information is summarized in the previous section of this appendix and on Table 1. Ideally, there would be independent information for each of these values and together they would be consistent with the geologic slip rate (rupture displacement * recurrence interval = slip rate). Unfortunately, many segments have few or no data, and existing data are often inconsistent. To deal with this situation, an effort was made to determine which pieces of data are most reliable for each segment, and either calculate the other values needed or modify the lesser quality estimate to be more consistent with the higher-quality data. In general, it is rare to have more than 1 or 2 displacement measurements, whereas many sites have recurrence information spanning 3-15 events. Generally, the recurrence interval was determined first, and then compared to the slip rate and displacement data (if available). If the data were reasonably consistent (inferred recurrence calculated from the single event displacement and slip rate were similar to the recurrence data), the observed recurrence interval was used. Alternatively, if displacement data were judged to be more reliable than the recurrence data, or recurrence data were unavailable and only displacement and slip rate data were available, the recurrence interval was calculated from the displacement data and the slip rate.

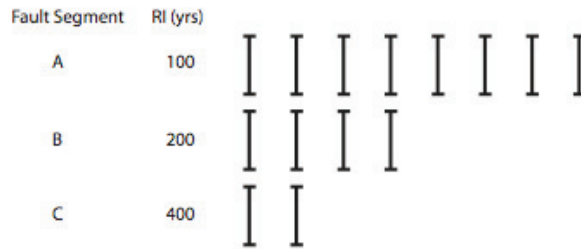
Finally, if there were no displacement or recurrence data for a segment, values from adjacent or similar segments were used or were calculated from the slip rate, the surface area of the segment, and scaling relationships relating rupture displacement to the surface area of rupture. In some cases, values were simply accepted from previous Working Groups, which implicitly or explicitly made similar calculations. This was done in a very qualitative manner at our San Diego meeting and later compiled by Ray Weldon in the *A_FaultsSegmentData* excel table, available from the WGCEP website (www.wgcep.org).

Many of the segments have only a few observations of displacement or recurrence intervals; therefore the values calculated may not adequately define the actual range of values. Because of this, we expanded the range of values generally to include the longest and shortest intervals or largest and shortest displacements observed. Considerable “geologic insight” is required to infer the quality of the data, so each value was discussed and generally the geologist most familiar with the data was called upon to defend the range of values chosen.

Once the data were assembled, “maximum,” “minimum,” and “geologic insight” models were constructed. Maximum refers to the model that produces the greatest number of earthquake ruptures to honor the recurrence intervals, and was generally constructed by allowing every segment to rupture independently. A minimum-ruptures model was constructed by assigning the longest-possible rupture, usually the entire fault zone, using the shortest recurrence interval consistent with all of its component segments. The next-longest rupture was constructed from the remaining recurrence intervals, and so on until all of the earthquakes were accounted for.

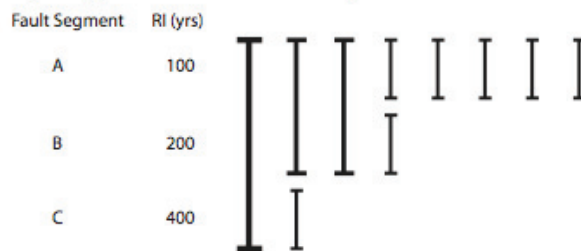
The easiest way to envision this is by hypothetical example, illustrated on Figure 1: Imagine a fault with 3 segments: A, B, and C, with recurrence intervals of 100, 200, and 400 years, respectively. In a maximum earthquake model that satisfies the recurrence data, the fault would have seven earthquakes every 400 years, with each earthquake occurring on a single segment: Four earthquakes on segment A, two earthquakes on segment B, and one earthquake on segment C. Figure 1 shows this as the individual segments each rupturing individually honoring the segment recurrence intervals.

Maximum earthquakes model: 14 events in 800 years



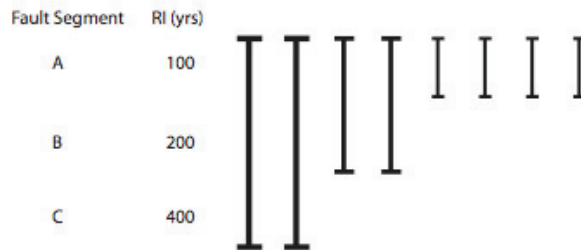
*The maximum earthquakes model is constructed by allowing all segments to slip independently.

Geologic insight model: 10 events in 800 years



- Segment B has large slip-per-event for the most recent event, so it is inferred that the rupture crossed over into adjacent segments A and C.
- Timing of events is indistinguishable for two events between segments A and B. Additionally, B has failed once during a period when A and C had no events. Based on event timing, segment C has also failed alone for one event.
- Segments A and B share a similar slip rate; however, small displacements per event of segment A suggest that it fails more frequently (five more earthquakes) than the adjacent segment B.

Minimum earthquakes model: 8 events in 800 years



*Minimum earthquakes model assigns as many paleo-earthquakes as possible to the longest possible rupture; in this case A+B+C; this covers all paleo-earthquakes on segment C. Next, as many paleo-earthquakes as possible are assign to the next largest rupture, A+B; this covers all paleo-earthquakes on segment B. Finally, the remainder must be only A.

Figure 1. Illustrated example of the Maximum, Geologic Insight, and Minimum earthquakes models. Lines represent single or multi-segment ruptures, corresponding to the fault segments labeled A, B and C.

In a minimum earthquake ruptures model, the segments can be combined so the fault would have four earthquakes every 400 years: One earthquake involves segments A+B+C. Another earthquake involves A+B, and there are two additional segment A-only ruptures. Figure 1 illustrates how the segments either rupture individually or link up in different combinations to produce the fewest number of ruptures that honor the segment recurrence intervals.

The “geologic insight” model was constructed by evaluating the likelihood of all single and multi-segment ruptures using the data on recurrence, event timing, slip rate, and slip-per-event. This was iteratively combined so that all of the recurrence data were satisfied. This is a qualitative process informed by different geologists’ opinions of the significance of segment boundaries, similarity of the timing and size of displacements between adjacent segments, extent of historic ruptures (if any), and other insights or biases based on their experience with the fault in question or other faults inferred to behave in a similar manner. Figure 1 shows this by listing the different types of paleoseismic data available that would influence how the geologic insight model could be constructed.

For example, in the hypothetical geologic insight model of Figure 1, the “available” paleoseismic data suggests that 1.) Segment B had a large average slip during the most recent event and this inferred large earthquake (large slip = bigger earthquake) likely ruptured onto the adjacent segments, leading to at least one earthquake that ruptures the full fault length. 2.) The timing of two events on segments A and B are indistinguishable. Also based on timing, it can be shown that B failed once by itself and C failed once by itself. 3.) Although segments A and B share a similar slip rate, slip per event on segment A is smaller, indicating that earthquakes on segment A are more frequent than on segment B.

Generating rupture rates from these geological insights was done by dividing each recurrence interval into a sufficiently long period of time and dividing up the number of earthquakes for each segment. In this example, C ruptures twice: once as A+B+C (1/800) and once as C (1/800) independently in an 800 year period. Segment B+A fails twice together in 800 years (2/800), leaving B to fail once alone (1/800) and A to fail five times alone during the 800 years (5/800). The total rate of earthquakes along the fault is 10/800 years, which is intermediate between the minimum rate model of 4/400 (8/800) years and the maximum model of 7/400 years (14/800) years. While this appears convoluted and imprecise, it was easy to implement and various possibilities were built, discussed, approved, or rejected until the geologic consensus or “insight” model was constructed.

After these crude ratios were constructed, exact values consistent with the slip rates were calculated in an Excel spreadsheet (see the *A_FaultsSegmentData* excel table at www.wgcep.org). Also, it was decided subsequently that every combination was possible at some low level, all of the geologic insight models were modified to allow for some small possibility that any rupture combination could occur. If there were no data to constrain this possibility, then it was assigned a rate of 50% of the lowest rate value in the geologic model. The 50% value was selected to allow for some possibility that the rupture could occur, but much less likely than the smallest value of what is constrained by the geologic data available. If some geologic data was available to suggest the possibility of a rupture combination was unlikely, then a “10%” rule was applied. The idea was that there are some rupture possibilities that are considered highly unlikely based on geologic insight, but we did not want to zero them out entirely. Thus, the 10%-rule ruptures are inferred to be less likely than the combinations that had the “50%” rule applied. In the example above, the combination BC would be added, given the weight of 1/8000, and the other rates adjusted slightly so the total RI on each segment remained the same. These adjustments are done in the inversion using the *A_FaultsSegmentData* table. Rupture combinations where the 50% rule are applied have a value of -1 in the table, combinations that have the 10% rule applied to them are coded with a value of -2. Finally, it should be noted that these *a priori* rupture

models are not moment balanced. This is done in the inversion and the process and results of the moment balancing are described in Appendix G.

In the following sections, we describe the basic geologic data that define these fault segments. The data included in this discussion are organized by fault and include slip rate, event chronology including mean recurrence, event ages and timing of the most recent event, and slip-per-event data where available. After discussion of the basic geologic data, we describe minimum-, maximum-, and geologic-insight-rate models for the Elsinore, San Jacinto, and Garlock faults. While the minimum and maximum rate models are relatively straightforward in how they are constructed (although not necessarily always plausible), the geologic-insight model is not quantifiable, nor necessarily unique, and represents the expert opinion of how the fault likely behaves by those who constructed the models using the available data.

Elsinore Fault

The Elsinore fault extends for nearly 200 km from near the border with Mexico to its northern termination near Whittier Narrows (Figure 2). WGCEP 95 describes five fault segments that are adopted by this working group. These are, from north to south, the Whittier, Glen Ivy, Temecula, Julian, and Coyote Mountains segments. These segments are assembled from seven fault sections in the Fault Section Database 2.0. The “Glen Ivy stepover fault section” and the “Temecula stepover fault section” are distinct sections, because the faults slip rate is split between the two parallel sections, but they are not segments (i.e., independent rupture sources). Because the Laguna Salada fault is classified as a “B-fault” we did not consider it in our rupture models for the Elsinore fault system. The geologic data for each segment are described below.

Whittier Segment. We adopt the WGCEP 95 description of the Whittier section of the Elsinore fault as extending 25-30 km from the Whittier Narrows south to the Santa Ana River. The Whittier segment is defined by changes in fault geometry between it and the Glen Ivy section to the south. These changes include a gradual 20 degree bend to the northwest from about N50W along the Glen Ivy segment to ~N70W, and a change in dip orientation from 80° SW along the Glen Ivy segment to 70-75° NE along the Whittier segment (Wills and others, 2007).

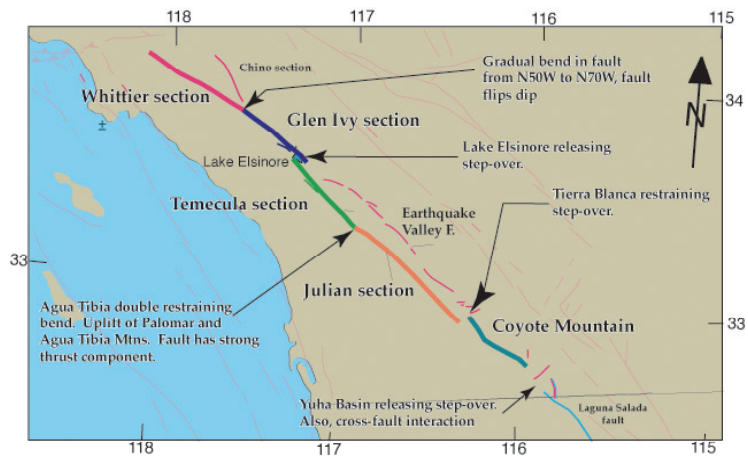


Figure 2. Location map for the Elsinore fault showing fault sections and geometric discontinuities.

Three-dimensional trenching at two sites provides a minimum geologic slip rate for the Whittier segment of the Elsinore fault. Rockwell and others (1992) determined a minimum slip rate of 2.5 – 3.0 mm/yr near Yorba Linda using offset channels incised into a fan that was dated using radiocarbon. At Olinda Creek near Brea, Gath and others (1992) resolved a minimum slip rate of about 1 mm/yr over the past 14 ka across one fault strand at the site. Another nearby fault strand shares a similar geomorphic expression and similar-sized stream deflections, suggesting a minimum rate for the two main strands of about 2 mm/yr. These minimum slip rates were

considered by WGCEP 95, and the preferred 2.5 ± 1 mm/yr slip rate for this segment is adopted here.

Three-dimensional trenching also provides constraints on slip during the most recent event (MRE), as documented by Patterson and Rockwell (1993) and Weldon and others (1996). In this study, slip during the MRE is resolved to be 1.9 ± 0.1 meters of right-lateral slip across one strand. This is considered to be a minimum because slip during this event is unresolved on another strand of the fault, which may have moved during the same earthquake.

The limited information available on the timing of paleoearthquakes on the Whittier segment is based on paleoseismic studies at the Olinda Oil field site. Patterson and Rockwell (1993) constrain the timing of the MRE to be between 1400-2200 years ago. The penultimate earthquake is constrained to have occurred less than 3400 years ago, possibly between 3000-3100 years ago, based on two charcoal samples taken from above and below the event horizon with nearly identical ages. However, the event age is likely unconstrained on the younger end and assumes that the charcoal sample taken from above the event horizon does not have an inherited age. This provides limited information on recurrence with one interval that is between 800-2000 years. The open interval between the MRE and the present is between 1400-2200 years, which is similar to the interval between the MRE and penultimate (PEN) events.

WGCEP 95 estimated a minimum recurrence interval using the slip rate of 2.5 ± 1 mm/yr and the minimum slip-per-event of 1.9 ± 0.2 m to obtain a calculated recurrence interval of 760 (+640, -275 yrs). This recurrence is on the low end of the one interval that is constrained in the paleoseismic record as well as the open interval of 1400-2200 years since the MRE. Although the available data only provide recurrence information based on one interval plus the open interval since the MRE, we use the interval-derived recurrence of 800-2000 years as an alternative to the recurrence used by WGCEP 95 for the Whittier segment.

Glen Ivy Segment: The Glen Ivy segment is located between the southern end of the Whittier segment and the ~ 2.5 km-wide Lake Elsinore releasing stepover that separates the Glen Ivy segment from the Temecula segment to the south. This segment includes the Glen Ivy and Glen Ivy stepover fault sections, for a segment length of about 40 km.

A preferred slip rate of 5.3-5.9 mm/yr, with a possible range of 2.6-9.3 mm/yr, is documented by Millman and Rockwell (1986) and is based on correlating offset alluvial fan deposits. Age control is based on soil development, and radiometric age control is not available. The fault section database uses a value of 5 ± 2 mm/yr to capture a preferred value and an uncertainty around the reported range. We adopt this rate for the purposes of constructing the rupture models described later.

Slip-per-event is based on a buried cultural feature that was offset about 25 cm during the MRE, inferred to be surface rupture from the May 15, 1910 earthquake (Rockwell, 1989). However, based on amounts of relative deformation observed in the trenches, it is inferred that some events prior to the MRE have produced larger amounts of slip than the 1910 earthquake. The slip-per-event for the events inferred to be larger than 1910 is unconstrained. The only other observation of slip-per-event is that slip across a secondary fault strand in the \sim A.D. 1280 earthquake was ~ 50 cm (Rockwell, 1989). Because this occurs across a secondary fault strand, this is regarded as a minimum, as well. We infer that the Glen Ivy segment appears to have a bimodal slip style, and that half of the ruptures appear to have 10's of centimeters of displacement (similar to the 1910 earthquake) and are classified as a sub-segment, whereas others appear to have larger (but

exact value unknown) earthquakes that may include the entire segment, and possibly adjacent segments.

Paleoearthquake timing and mean recurrence are the most robust paleoseismic data for the Elsinore fault along the Glen Ivy segment (Rockwell and others, 1986). An average recurrence interval is based on 6 events (5 intervals) and the use of the latest radiocarbon dating and models of event chronology constructed in OxCal, we calculate a mean recurrence between 159-189 years for the past 794-947 years (See *Appendix B: Recurrence and Event Ages* for a full listing of event ages and recurrence). However, unpublished data by Rockwell suggests that half of the six events are larger than the 1910 earthquake, based on relative amounts of deformation. We adopt a recurrence interval for the inferred larger events of 384 years (288-480 years). This is using the three events (two intervals) that are inferred to carry most of the slip and that post date A.D. 900-1075 and predate the historical record starting in A.D. 1850. Some of these data have not been published or formally reviewed.

Temecula segment: The Temecula segment extends for a distance of about 50 km between the Glen Ivy stepover on its northern end to the Agua Tibia double restraining bend. The double restraining bend at Agua Tibia Mountain forms the boundary between with the Julian segment to the south.

Rockwell and others (2000) report a late Holocene slip rate of $4.9^{+1.0}_{-0.6}$ mm/yr. This is based on an offset channel displaced 9.8 ± 0.5 m during the past 2000 years. The age control for this offset is a sample of charcoal that constrains the age of the channel to be 1954^{+185}_{-134} calibrated yrs B.P. (pre-1950 A.D.).

Based on studies at two trench sites located on the Temecula segment near Agua Tibia Mountain, Vaughan and others (1999) identified four events in the paleoseismic record that occurred between 2.7 ka and just before 4.5 ka. Assuming that the record is complete for this period of time, average recurrence (3 intervals, two actually constrained) is about 400-600 years. The paleoseismic record for the period after 2.7 ka is incomplete, but the timing of the most recent event is constrained to be between A.D. 1655 and A.D. 1810. The constraints are based on radiocarbon dating for the older end of the event age range and the historic record at the onset of construction at the Pala Mission complex in about A.D. 1810.

There is no independent slip-per-event information available for this section of the Elsinore fault. However, slip per event can be inferred from frequency and slip rate. Using a preferred mean recurrence of 600 ± 150 years and a slip rate of 5 ± 2 mm/yr gives a slip-per-event estimate of about 3 (+2.25, -1.65) m.

Julian segment: The Julian segment is the longest individual segment of the Elsinore fault zone, extending southward for 65-75 km from the double restraining bend at Agua Tibia Mountain to the 4- to 5-km-wide extensional step to the Coyote Mountains segment. Studies of microseismicity (Magistrale and Rockwell, 1996); Nazareth and Hauksson, 2004) suggest a larger down-dip width than for other sections of the Elsinore fault, based on deeper seismicity. This suggests that earthquakes along this segment may be larger than generated by other parts of the Elsinore due to a larger down-dip width and rupture length.

The Julian segment is notable for its lower slip rate of ~ 3 mm/yr (2.5-3 mm/yr) compared to the higher value of around 5 mm/yr to the north along the adjacent Temecula segment. This lower slip rate is based on a long-term (900 ka) geologic offset described by Magistrale and Rockwell

(1996), based on the initiation of activity along the Elsinore fault between Palomar Mountain and the Vallecito-Fish Creek Basin. This lower slip rate may be due to partitioning of the total slip budget between the Julian segment and the Earthquake Valley fault to the east which likely takes up the remaining amount of total slip within the fault system. The fault section database reports a slip rate of 3 ± 1 mm/yr for the Julian segment, which is similar to the reported geologic values, but with larger uncertainty. There are no slip-per-event data available for this section of the fault.

Information about timing and earthquake recurrence along the Julian segment is limited to a two-event record at the Lake Henshaw trench site, supplemented by another trench near Julian (Thorup, 1997). At Lake Henshaw, two events were identified and their timing was constrained by radiocarbon dating to be between 1.5 and 2.0 ka for the MRE and 4.0 and 6.0 ka for the penultimate event. At the Julian site, 12 km to the south, the timing of the MRE was between 0.7-1.7 ka. Due to the close proximity of the two trench sites, Thorup (1997) suggested that the MRE at both sites is the same earthquake, and that the timing is better constrained at the Julian site. The nature of the trench sites allows for missed events, but events appear to be less frequent on the Julian segment relative to other segments of the fault. Thorup (1997) estimate a recurrence interval for the Julian segment of 3000 to 3500 years between the two events seen in the trenches. This implies relatively large displacements if one assumes a slip rate of 3 mm/yr, which influences the construction of the rupture models, as described in the next section. Because of the potential for missing events and general lack of a paleoseismic record with more than two events, we assign a preferred recurrence of 1000-3000 years. The lower end of the range was assigned based on the open interval for the Julian segment, recognizing that the available data has large uncertainties.

Coyote Mountains segment: The 30- to 35-km-long Coyote Mountains segment is separated from the Julian segment by a left restraining stepover near the Tierra Blanca Mountains. The southern end of the fault is defined by a releasing step with several northeast-trending cross faults that separate it from the Laguna Salada fault, which continues southward into Mexico.

Pinault and Rockwell (1984) estimated a slip rate of 4 ± 1 mm/yr based on estimates of soil age of Holocene alluvial channel deposits offset about 40 m. More recent, unpublished estimates by Rockwell (personal communication, 2006) constrain this to be closer to 3 ± 1 mm/yr, which is the value in the fault section database. Slip-per-event data are remarkably robust for this segment. Well-preserved offset gully and channel gravel bars along the fault show that slip from the most recent event varied from 1.5 meters along the southern part of the fault to a maximum of 2.9 meters along the central part of this segment. Slip during the inferred penultimate event appears to be similar to slip in the MRE (Rockwell, 1990). However, he notes that slip during the third event back may have been smaller than slip during the MRE.

Recurrence data for this part of the fault are based on three events during the past 2000 years, using TL dating of fissure fill material. Based on unpublished event dating, the recurrence is between 800 and 1000 years the since 2 ka (Tom Rockwell, written communication).

Elsinore Fault Rupture Models

We use the following abbreviations for the different fault sections in the following discussion: W = Whittier, GI = Glen Ivy, T = Temecula, J = Julian, CM = Coyote Mountains.

Minimum Ruptures Model: Following the general scheme described above, we first made the minimum number of scenarios that satisfied the recurrence data. The minimum rate model for the Elsinore fault allows for the following possibilities: CM+J+T+GI+W, CM, T+GI+W, T+GI, and GI. This essentially corresponds to about 16-17 ruptures over 4000 years in our assigned rate column on Table 1.

Maximum Ruptures Model: The maximum rate model for the Elsinore fault is the simple end-member model that allows for each segment to rupture independently (W, GI, T, J, and CM). The available data allow for this possibility, although it was considered unlikely by the geological working group.

Geologic Insight Model: The geologic insight model was constructed using the geologic data described previously. The geologists produced seven likely ruptures that honor the recurrence data. The different rupture scenarios and reasons for combining them are described below:

CM+J+T+GI: Scenario CM+J+T+GI is the model with the maximum number of fault segments breaking simultaneously in the geologic insight model. This scenario was created on the basis of paleoseismic data that suggest that full Elsinore ruptures may not occur given that the Glen Ivy (GI) segment of the Elsinore fault has failed at least six times during the past 1000 years without the Whittier segment failing during the same period of time, as the most recent event on the Whittier is thought to be between 1400-2200 years ago. A 20-degree change in strike, as well as a change in dip direction between the Whittier and Glen Ivy sections, also influenced the decision that full Elsinore fault ruptures are unlikely in the geologic insight model.

Unfortunately, a complete paleoseismic record for the Glen Ivy segment that overlaps with the timing of the MRE on the Whittier segment does not exist. This leaves open the possibility, although it was considered unlikely, that the Whittier and Glen Ivy have failed together in the past.

CM+J+T: Scenario CM+J+T is based mostly on paleoseismic and seismological constraints along the Julian segment. Here, the geologists felt that the long recurrence interval for the Julian segment, (2 events identified in the past 6000 years), a 3 mm/yr slip rate, and larger down-dip width of the fault would produce infrequent, but large earthquakes. These inferred large earthquakes suggest that ruptures on the Julian segment could propagate onto the adjacent segments. Thus, in this model, a rupture on the Julian segment of the fault will continue to adjacent segments and the segment would be less likely to fail by itself.

CM and T (individually): Using the recurrence information, which suggests the Julian segment fails far less frequently, the geological insight model proposes that the Coyote Mountains and Temecula segments can each fail individually, with the Julian segment acting as a barrier between the two. For the Coyote Mountains, the recurrence data shows that it has failed more frequently (3 events in 2000 years) with smaller slip-per-events than what is inferred for the adjacent Julian segment. The Temecula segment shares similar characteristics of more frequent ruptures (RI: 450-700 years) than the Julian segment and assumed smaller slips-per-event (~3m) which suggests that it too may fail independently of the Julian segment.

T+GI: While the Temecula segment can fail independently of the Julian segment, it may also rupture with the Glen Ivy segment. This is permitted by the data, as the Glen Ivy segment fails frequently relative to the Temecula segment. This possibility is supported by some event timing information. The MRE for the Temecula segment (AD 1650-1810) overlaps with the penultimate event at Glen Ivy Marsh, dated between AD 1627-1836.

GI: Glen Ivy is treated as a segment that is capable of rupturing individually based on several lines of evidence. A moderate sized (M6?) historical event in 1910 only ruptured the GI segment of the fault, producing about 25 cm of right-lateral displacement at Glen Ivy Marsh. Also, the Glen Ivy segment has a shorter average recurrence (6 events in 1000 years, including minor events) than the adjoining Whittier and Temecula segments, another indication that it fails more frequently than the adjacent segments.

W: The geologic insight model treats the Whittier segment as being capable of only failing independently. The Whittier fault has not failed for the past 1400 years, while the adjacent Glen Ivy segment has failed multiple times during the past ~1000 years. The lack of interaction between the Whittier segment during a period when the adjacent Glen Ivy segment has failed multiple times is one line of reasoning that the Whittier segment only fails independently in this geologic insight model. Also, the geologists involved with creating the geologic insight model considered the 20-degree change in fault trend, as well as change in fault dip between the Whittier and Glen Ivy segments as features that could inhibit ruptures from propagating into or out of the Whittier segment.

San Jacinto fault

The San Jacinto fault zone is one of the most seismically active faults in California, in terms of both its microseismicity and the moderate and large earthquakes that it has produced in the historic record. The fault zone stretches from its junction with the San Andreas fault near Cajon Pass to the Imperial Valley for a distance of ~250 km. Since the 1988 WGCEP, the fault has been divided into different segments based on fault geometry, historical seismicity, and slip rate data. The fault is divided into eight segments, assembled from the eleven sections described in Fault Section Database 2.0. The San Jacinto fault zone is divided into San Bernardino Valley, San Jacinto Valley, Anza/Clark, Coyote Creek, Borrego Mountain, and the sub-parallel Superstition Mountain and Superstition Hills segments (Figure 3). These are individual sections from the fault-section database, with the exception of the San Jacinto Valley segment, which includes the San Jacinto Valley and San Jacinto Valley stepover sections, and the Anza/Clark Segment, which includes the Anza stepover, Anza, and Clark sections. For the rupture models that were developed, little was changed from previous segmentation schemes although we did not consider the Superstition Hills segment in our rupture scenarios.

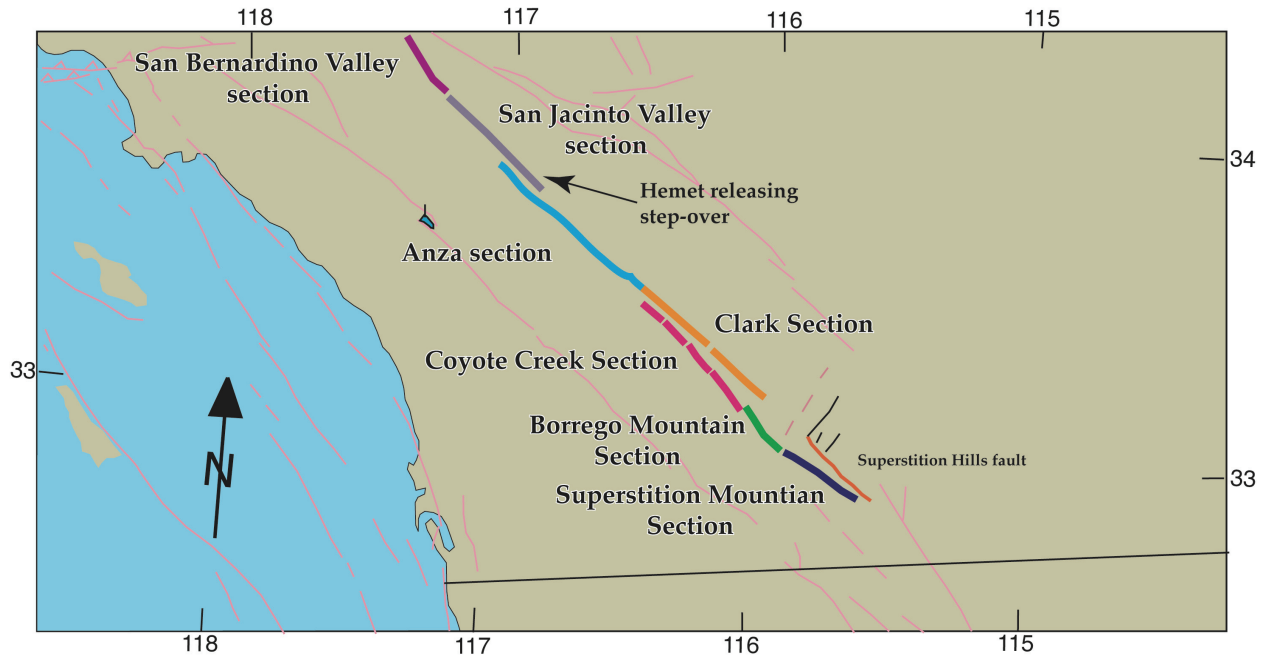


Figure 3. Location map for the San Jacinto fault showing fault sections and geometric discontinuities.

San Bernardino Valley segment: The 35- to 40-km-long San Bernardino Valley section extends from the San Jacinto fault's northern termination near the San Andreas fault to the northern San Jacinto Valley. Few geologic data exist to constrain a slip rate along the San Bernardino Valley section of the San Jacinto fault. A geologic slip rate of ~ 2.5 mm/yr is reported across the Lytle Creek strand of the fault (Mezger and Weldon, 1983). This is a minimum rate for the entire zone. Wesnousky (1986) estimated a slip rate of 8-12 mm/yr, based on a synthesis of geologic, geodetic, and seismological data. A slip rate of 12 ± 6 mm/yr is inferred and used by WGCEP 1995, by extrapolating the slip rate measured along the Anza segment by Rockwell and others (1990) northward to include both the San Jacinto Valley and San Bernardino Valley sections. Higher slip rates, ~ 17 mm/yr over the past 0.7 m.y., are suggested by Morton and others (1986). Kendrick and others (2002) have modeled slip rates >20 mm/yr based on uplift rates during the past 100,000 years. The current WGCEP has proposed two possible slip rates for this section of the fault in the deformation models, one using the WGCEP 95 slip rate of 12 ± 6 mm/yr and an alternative higher slip rate of 18 ± 6 mm/yr that is based on a combination of geologic and recent geodetic studies as described by the Fault Section Database (see www.wgcep.org).

Preliminary recurrence data from the Walnut paleoseismic site suggests the average interval between earthquakes is between 132-287 years (Appendix O, this report). This is based on a paleoseismic record of six events in a ~ 1000 year interval between 3.0 and 4.0 ka (Fumal and Kendrick, personal communication). The Colton site, located about 7 km southeast of the Walnut site revealed two events in the past ~ 300 years (Kendrick and Fumal, 2005). Individual age constraints for these two earthquakes are not available.

San Jacinto Valley segment: The San Jacinto Valley section, which includes the Claremont fault, extends 40-45 km from a restraining bend at the northern end of the San Jacinto Valley along the east side of the Hemet releasing stepover. The Casa Loma fault, on the west side of the stepover, is considered to be part of the Anza segment.

Much like the San Bernardino Valley section of the fault, the San Jacinto Valley section has no geologically constrained slip rate and limited information on event timing. WGCEP 95 extrapolated the slip rate from the Anza section to include the San Jacinto Valley section. Wesnousky and others (1991) report a minimum rate of 1.7-3.3 mm/yr for the Claremont fault. However, this site is located on the San Bernardino segment of the San Jacinto fault and may or may not reflected the slip rate of the fault on the San Jacinto Valley segment. The fault section database assigns the same alternative ranges as for the San Bernardino Valley section of the fault: A slip rate of 12 ± 6 mm/yr is one alternative, while 18 ± 6 mm/yr is the other alternative, which uses the same rationale as the alternative slip rates that are assigned to the San Bernardino Valley section of the fault.

There are no paleoseismic data available to constrain event timing on this section of the fault, or the age of the most recent surface-rupturing event. However, the fault has been a source of significant earthquakes during the historic period. Bakun (2006) summarizes the evidence for the two significant earthquakes in 1899 (M6.9) and 1918 (M 7.1) that were located near or on the fault. Surface rupture was not documented for either of these earthquakes, thus even the timing of the most recent event is uncertain for this section of the fault. Rasmussen (1982) suggests that, even though no surface rupture was documented in 1918, surface rupture could have occurred along the Claremont fault because this fault strand was not investigated following the earthquake, thus putting the 1918 earthquake on the San Jacinto fault. There is no information on slip-per-event available for this section of the San Jacinto fault.

Anza/Clark segment: The Anza section extends for a distance of about 110 km from the Hemet releasing stepover south. Along the southernmost 50 km, the fault is also known as the Clark fault, and it parallels the Coyote Creek section for much of this distance. There are several mapped cross faults and transfer structures that appear to accommodate the transfer of slip across the boundary. For the purposes of considering various rupture scenarios, the Anza and Clark sections are combined from the fault section database and referred to as the Anza segment here. WGCEP 95 also combined these sections into one segment, although not explicitly for the purpose of considering rupture scenarios.

The Anza segment has the most robust paleoseismic dataset of any segment of the San Jacinto fault. These data constrain both mean recurrence as well as slip rate. Rockwell and others (1990) used dated offset alluvial fans of Late Pleistocene and Holocene age near Anza to estimate a slip rate of $12 (+7, -5)$ mm/yr. The most recent work at the Hog Lake paleoseismic site suggests a ≥ 16 mm/yr slip rate for a late Holocene fan offset at least 28 m since A.D. 300 (Rockwell and others, 2006). Janecke and others (2005) document a long term (0.5 Ma) slip rate of 10 mm/yr for the Clark strand and a 5 mm/yr slip rate for the Coyote Creek strand, giving a slip rate of about 15 mm/yr for the system.

Slip-per-event data for this section of the fault are also available for the most recent event and provide a paleo-slip distribution for the most recent event along the southern part of the Anza section to at least the Hog Lake area (Middleton and Rockwell, personal communication). Slip-per-event was about 3-4 meters during the most recent event, with the maximum slip occurring near the Hog Lake site. Mapping north of the Hog Lake site has not been completed, but assuming that slip tapers down from a peak near Hog Lake, these observations suggest that most of the Anza segment of the fault may have ruptured during the MRE.

The Hog Lake paleoseismic site provides a record of at least 16 events identified in trenches that have occurred during the past 3.5-4.0 ka, indicating an average recurrence of 220-260 years (Rockwell and others, 2006). The timing of the MRE is no younger than A.D. 1800, and probably between A.D. ~1750-1800.

Coyote Creek segment: The Coyote Creek segment is about 40 km long, paralleling the Clark fault for much of this distance. The southern end of the segment is located at the northern end of the rupture zone of the 1968 M_w 6.5 Borrego Mountain earthquake.

There is currently short term (<10 ka) estimate of slip rate for this segment of the San Jacinto fault zone. Janecke and others (2005) estimate a slip rate of approximately 5 mm/yr for the Coyote Creek segment over the past 0.5 Ma. WGCEP 95 assigned a slip rate of 4 ± 2 mm/yr, which was extrapolated from the Borrego Mountain segment and is now adopted in the fault section database.

No data are available for recurrence along the Coyote Creek segment of the San Jacinto fault. Slip-per-event is estimated using slip from the 1968 Borrego Mountain earthquake (~50 cm), although new data being developed by Verdugo and others (2006) along the north break of the 1968 rupture suggest that the 1968 earthquake may be atypical for this part of the San Jacinto fault zone, with slip-per-event as high as 2.5 meters in previous events (personal communication). This would suggest that ruptures may not be limited to the extent of surface rupture seen in 1968 along the Borrego Mountain segment, but instead extend into the Coyote Creek segment of the fault. We assign a recurrence range of 125-625 years, which is calculated using the preferred slip rate and the range of the slips-per-event described above. This range could be reduced by assuming that 1968 was not the characteristic earthquake.

Borrego Mountain segment: The Borrego Mountain segment is defined by the extent of faulting observed following the M 6.5 1968 Borrego Mountain earthquake, which ruptured 31 km of the San Jacinto fault. Surface slip during this earthquake reached a maximum of 38 cm of right-lateral offset.

A slip rate of 2.8-5.0 mm/yr was published by Sharp (1981) based on a 1.7 m offset of a Lake Cahuilla shoreline dated to 275-510 yrs BP. Another short-term slip rate for the past 300 years is based on 1.4 meters of slip on a Lake Cuihilla gravel bar and gives a slip rate of about 4.5 mm/yr (Pollard and Rockwell, 1995). WGCEP 95 and the fault section database adopt a slip rate of 4 ± 1 mm/yr which covers the range of reported slip rates.

A minimum recurrence of 60 years is from Pollard and Rockwell (1995), assuming 1968-type events are typical. An upper limit of recurrence is about 200 years and is adopted from studies by Clark and others (1972). However, the paleoseismic site of Clark and others (1972) may lack the stratigraphic resolution to detect all earthquakes, thus the paleoseismic record represents a minimum number of events at their site.

Superstition Mountain segment: The Superstition Mountain segment of the San Jacinto fault zone extends for a distance of 25 km from the southern end of the 1968 Borrego Mountain rupture to the end of its mapped trace. The sub-parallel Superstition Hills segment, which ruptured in the M_w 6.6 1987 Superstition Hills earthquake, extends about 13 km farther south than the Superstition Mountain segment and is the southern-most mapped trace of the San Jacinto fault zone.

Verdugo and others (2006) propose a slip rate of 6 mm/yr during the past 1200 years. This is based on a buried channel offset 7 m during the past four events. A younger channel is offset 5.5 meters by only 3 events, gives an estimate of slip during the fourth event back of about 1.5 meters. Slip during the most recent event is about 2.2 meters of right-lateral offset (Gurrola and Rockwell, 1996). This is similar to geomorphic offsets observed along Superstition Mountain that range between 2.5-4 meters, and probably represent offset during the past 1-2 earthquakes (Rockwell, written communication).

Recurrence along the Superstition Mountain section of the fault is based on the work of Gurrola and Rockwell (1996). Based on the radiocarbon dates that were recalibrated in OxCal, we calculate a recurrence interval of 240-410 years for the past four events. The open interval since the most recent earthquake is about 500 years; this appears to be longer than the calculated average recurrence.

San Jacinto Fault Rupture Models

The following abbreviations are used for the San Jacinto fault zone: SBV = San Bernardino Valley, SJV = San Jacinto Valley, A = Anza-Clark, CC = Coyote Creek, B = Borrego, SM = Superstition Mountain.

Minimum Ruptures Model: The minimum ruptures model consists of the following combinations: SBV+SJV+A, A+CC+B+SM, B, B+SM. In this case, a full fault rupture was not considered as the group thought that the step between the A and CC would prevent the fault from failing in its entirety. This assumption is supported by the observation that, historically, faults have not ruptured through steps of ≥ 5 km-wide (Wesnousky, 2006). The historic 1968 earthquake allows for the Borrego Mountain segment to fail independently in this model. Paleoseismic data on timing and slip-per-event suggest that the Superstition Mountains section typically fails with the adjacent Borrego Mountain segment and probably does not fail by itself.

Maximum Ruptures Model: The maximum ruptures model involved each of the segments rupturing independently.

Geologic Insight Model: Along the San Jacinto fault, the limited number of paleoseismic data hinders the ability to make a well-constrained geologic insight model. Despite this, eight rupture scenarios are proposed using the slip rate, recurrence, slip-per-event, and fault geometry observations that are available:

SBV+SJV: Few paleoseismic data exist these segments. Although the moderate magnitude ($M \sim 6$) historical seismicity may reflect the typical behavior of this part of the San Jacinto fault, we do not consider in our scenarios as these have been less-than-full-segment ruptures. However, based on the geometry of the surface trace, there is little to suggest that the broad right bend in the fault would impede ruptures from propagating along the fault, thus the geologists felt that lumping these two sections was preferable than the segments failing independently.

A: Geometrically, the fault is straight and fairly continuous from the Hemet Valley stepover to where the fault steps over to the Coyote Creek section of the fault. Slip for the most recent event (MRE) has been recently mapped for the southern part of the fault using new LiDAR data. On the southern part of the Anza segment, from south to north, displacement in the most recent event ramps up to the 2-3 meter range, peaking at 3-4 meters at the Hog Lake paleoseismic site and averaging about 2.7 m along the length of the fault mapped for this project (Middleton and Rockwell, in prep). North of Hog Lake, displacement for the MRE has not yet been mapped, but

if slip continues and decreases gradually to the north, this would suggest that the MRE ruptured most of the fault between the Hemet stepover and the Coyote Creek fault.

SBV+SJV+A: Although the Hemet Valley ~5 km releasing stepover is significant (*e.g.* Wesnousky, 2006), this scenario was considered possible if a long, large-average-slip, Anza segment rupture occurred. Several cross-faults mapped in Hemet Valley suggest a possible structural connection at depth, allowing a rupture to propagate through the stepover in this scenario. No paleoseismic data that dates past earthquakes exist for the SBV+SJV sections to constrain this scenario.

CC: The Coyote Creek section of the San Jacinto fault is considered to be capable of rupturing independently under the geologic insight model. The ~40 km of historically unruptured fault section that lies between the Coyote Creek – Anza segment stepover and the northern extent of the 1968 Borrego Mountain earthquake is the basis for this possible scenario. Little paleoseismic data exists to constrain this. However, based on historical observations of surface-rupturing earthquakes, the > 5km stepover between the Coyote Creek segment and the Anza segment is thought to be large enough to restrict a rupture from propagating through to the Anza segment (Harris and Day, 1993; Wesnousky, 2006). Thus, the geologic insight model gives low (but not zero) weight to ruptures that cross this boundary.

B: The 1968 Borrego Mountain earthquake provides the historically observed constraint that allows for this part of the San Jacinto fault to fail independently.

B+SM and CC+B+SM: The Superstition Mountain section of the San Jacinto fault is the controlling section for these two scenarios. Slip-per-event of about 2.5 meters is observed along the Superstition Mountains fault based on geomorphology. A paleoseismically determined displacement of 2.2 meters for the MRE also suggests that this fault ruptures with larger slip-per-events than the Borrego Mountain section of the fault. This allows for the possibility that ruptures on the Superstition Mountain section of the fault bleed onto the Borrego Mountain section or even to the Coyote Creek section of the fault. Work in progress shows that there is evidence at two sites that suggests that events on the Superstition Mountain fault also involve the Coyote Creek fault (Verdugo and others, 2006). As mentioned previously, the geologic insight model considers it unlikely that ruptures would propagate through the Coyote Creek – Clark stepover, limiting the rupture to the southern three sections of the fault.

Garlock Fault

At the A-fault Rupture Modeling Summit meeting (June 12-14, 2006), the Garlock fault was added to the list of A-faults being considered by the WGCEP. The fault was divided into three sections: eastern, central, and western (Figure 4). The criteria for these sections are based on fault geometry and inferred slip rate and essentially follows the scheme of McGill and Sieh (1991) as well as the fault sections described in the U.S. Geological Survey Quaternary Fault and Fold Database. The eastern section of the fault extends for 50-60 km from near Death Valley westward to a significant change in strike from east-west to ~N64E. About five kilometers east of this change in strike, the northeast-striking Owl Lake fault branches away from the Garlock fault, apparently partitioning slip between the two faults, as suggested by McGill (1993). The central section of the fault extends westward from this segment boundary for a distance of ~110 km. Near the western end of the section is Koehn Lake, a 2-3 km-wide releasing stepover that defines the boundary between the central and western sections of the Garlock fault. The western

section of the Garlock fault zone extends nearly 100 km southwestward to the junction between the Garlock fault and the San Andreas fault near Frazier Mountain.

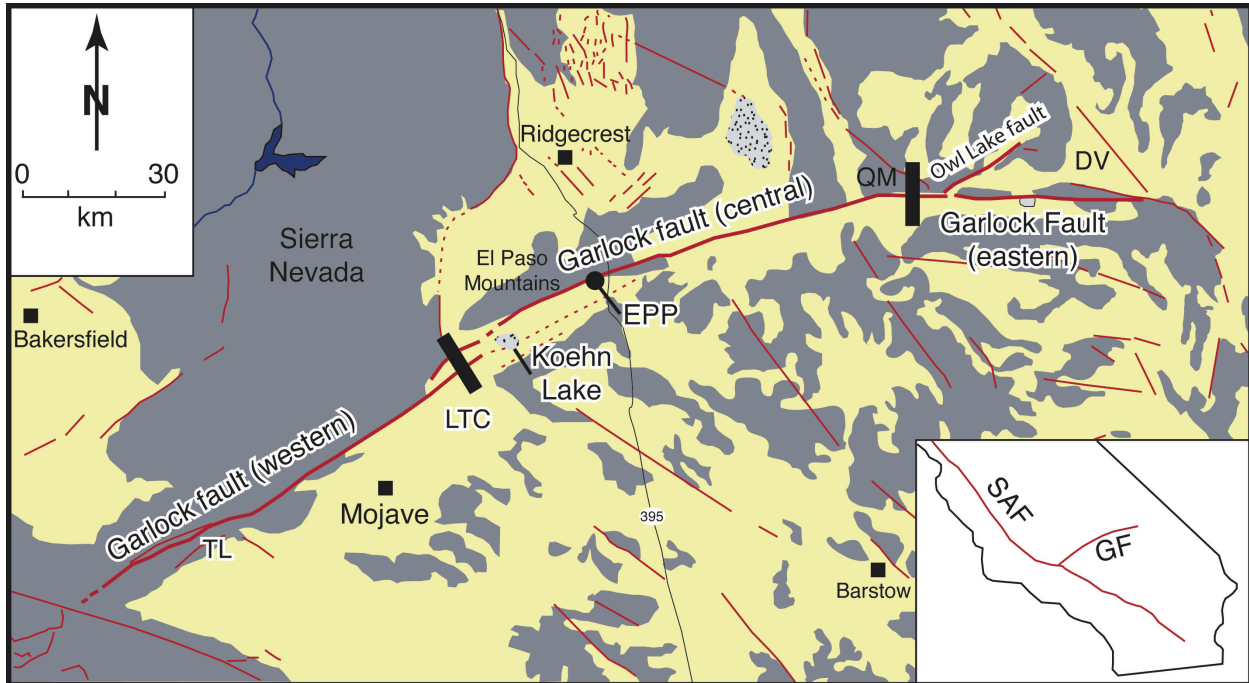


Figure 4. Location map for the Garlock fault showing fault sections defined by black bars. Bedrock is shown in grey fill, Quaternary fill is yellow fill. EPP is El Paso Peaks site, LTC is Lone Tree Canyon site, TL is Twin Lakes site, QM is Quail Mountains, DV is Death Valley. Modified from McGill and Sieh, 1991.

Eastern segment: Very little paleoseismic information exists to constrain slip rate for this section of the fault. However, McGill and Sieh (1991) infer some fraction of total slip is transferred to the Owl Lake fault, which has a preferred slip rate of 2.5 mm/yr (McGill, 1998). McGill and Sieh (1991) suggest a value of ~3 mm/yr for the eastern Garlock fault, based on this partitioning of slip to the Owl Lake fault. However, the assumed slip rate is poorly constrained and acknowledged to be somewhat uncertain (see discussion in Bryant, W.A., compiler, 2000, Fault number 69c, Garlock fault zone, Eastern Garlock section, in Quaternary fault and fold database of the United States: U.S. Geological Survey website, <http://earthquakes.usgs.gov/regional/qfaults>). Slip-per-event data for the easternmost Garlock appear to be the most robust geologic data available, with numerous geomorphic offsets clustering around 2.8 meters of left-lateral displacement in the eastern and western Avawatz Mountains (McGill and Sieh, 1991).

Information on event timing and recurrence data does not exist and is calculated from the inferred slip rate and slip-per-event data of McGill (1992). A mean recurrence of 933 years, listed in Table 1, is based on the slip-per-event of 2.8 m and a slip rate of 3 mm/yr.

Central segment: A preferred slip rate for the Central Garlock fault is fairly well constrained at 6 ± 1 mm/yr by McGill and Sieh (1993), with a total range of 4-9 mm/yr. This is consistent with other, less-well-documented slip rates such as the 5 - 8 mm/yr rate of Clark and LaJoie (1974), although as much as 11-12 mm/yr has been suggested (Carter, 1980, 1982). We adopt the preferred estimate of McGill (1992) as the slip rate for the central Garlock fault because it is the best-documented of the rates available in the literature.

Geomorphic offsets provide constraints on the slip-per-event for the MRE and prior events. Offsets for the inferred most recent event along the central section range from 7 meters along the western-most parts of the central Garlock to 2.0-3.5 meters in the Searles and Pilot Knob Valley areas (McGill, 1992). There are few geometric discontinuities along the Garlock fault to impede ruptures, suggesting that these offsets may be related to the same earthquake. The timing of the most recent earthquake at the El Paso Peaks site (Dawson and others, 2003) and in Searles Valley (McGill and Sieh, 1993), around the mid 16th Century, also suggests that these offsets may be related to the same earthquake.

Near El Paso Peaks, slip for the penultimate event appears to be about the same as that for the MRE, around 7 m of left-lateral slip, expressed as geomorphic offsets of about 14 m. It is possible that slip during the pre-penultimate event may have been less than that of the MRE and PEN, at ~4 meters. This inferred offset is based on a ~18 meter left-lateral offset that is inferred to represent cumulative slip over the past 3 events.

Average recurrence for this section of the fault is based on the identification of six paleoearthquakes that have occurred during the past 7000 years (Dawson and others 2003; McGill and Rockwell, 1998). A preferred mean recurrence of 1280 years is based on the six dated earthquakes during the past 7000 years. However, the individual intervals are noted to be highly irregular, ranging from as little as ~100 years to as much as 3000 years between earthquake.

Western segment: A recent study by McGill and others (2003, and manuscript in review GSA Bulletin) suggests that the slip rate for the eastern-most section of the western Garlock fault is 6.3 ± 2 mm/yr. McGill and others (2003) suggest a slip-per-event minimum of 2.75 - 3.75 meters per event based on a 2550 ± 200 yr BP age channel offset between 2 - 16 meters.

Recurrence data for the western Garlock fault are sparse, although trenching studies on the Tejon Ranch by Earth Consultants International indicates that there have been two events during the past 1700 years (Rockwell, written communication). A paleoseismic record at the Twin Lakes site by Madden and Dolan (in prep) reveals a preliminary record of four earthquakes since about 3620-3360 B.C. If the historic record is complete to about A.D. 1800 (assuming that a large, segment-rupturing earthquake on the western Garlock would be felt at the Spanish missions in the Los Angeles basin), the average recurrence for the western Garlock fault is >1000 years. Based on their work at the Lone Tree Canyon site, McGill and others (manuscript submitted to GSA Bulletin) infer an average recurrence between 1200-2700 years. We assign an average interval of ~1100 years, based on Madden and others (2005). However, we note that this data is being revised and will likely result in a slightly longer average interval (Madden and Dolan, written communication, 2007). Unfortunately, this data was not available to us before the ERM 2 was finalized and is not reported here, although this will likely be incorporated in future revisions of the ERM.

Garlock Fault Rupture Models

The following abbreviations are used for the Garlock fault sections: GE = Garlock east, GC = Garlock central, GW = Garlock west

Minimum Ruptures Model: The minimum ruptures model stipulates that a rupture can involve the entire fault length (GE+GC+GW). Based on historical examples, McGill and Sieh (1991)

suggest that the Garlock fault could rupture through the Koehn Lake stepover and produce a full fault-rupturing earthquake.

Maximum Ruptures Model: The maximum ruptures model involves each of the fault sections rupturing independently.

Geologic Insight Model: The geologic insight model proposes six rupture scenarios based largely on fault geometry, slip rate, and limited paleoseismic recurrence data:

GE, GC, GW (individually): Based on fault geometry and differences in slip rates, the Eastern (GE), Central (GC) and Western (GW) sections of the Garlock fault are considered to have the potential of failing independently. The ~3 km Koehn Lake stepover is a possible segment boundary between the western and central Garlock faults. A change to a more easterly trend, combined with the splaying off of the Owl Lake fault and inferred reduction of slip rate for the easternmost Garlock fault separates the central Garlock fault from the eastern section of the Garlock fault. These differences allow the inference that each of these sections may fail independently of each other.

GE+GC: The geologic insight model allows for the possibility of the central and eastern Garlock faults failing together. No event timing data exists to constrain this. However, geomorphic offsets that are inferred to be from the MRE along the eastern part of the central section and offsets along the eastern section of the fault are both around 3 meters, leading to the possibility that that these similar offsets along both sections may be from the same earthquake.

GC+GW: Similar slip rates on both sides of the Koehn Lake stepover, and a stepover width of <5 km that does not necessarily preclude ruptures from being arrested at the stepover (Wesnousky, 2006) leads to the possibility of a rupture that involves the central and western sections of the Garlock fault. A developing event chronology at the Twin Lakes site on the western Garlock fault (Madden and Dolan, in prep) and an established event chronology at the El Paso Peaks site on the central Garlock fault (Dawson and others, 2003; McGill and Rockwell, 1998) suggests that timing of at least some events between the two sites may overlap, allowing for the possibility that the two sites may see the same ruptures. Large geomorphic offsets of ~7 m inferred to represent slip during the most recent event (McGill and Sieh, 1993; Dawson and others, 2003) along the western-most part of the central Garlock fault may also suggest that ruptures may be large enough to cross the Koehn Lake stepover, involving both of these segments.

GE+GC+GW: Although unconstrained by paleoseismic data, the fault geometry of the Garlock fault may be simple enough to allow for large ruptures to propagate along the entire length of the fault.

References

- Bakun, W.H., 2006, Estimating locations and magnitudes of earthquakes in Southern California from modified Mercalli intensities: *Bulletin of the Seismological Society of America*, v. 96, p. 1278-1295.
- Carter, B.A., 1980, Quaternary displacement on the Garlock fault, California: in *Geology and Mineral Wealth of the California Desert*, edited by D.L. Fife and K.R. Brown, pp. 457-466, South Coast Geological Society, Santa Ana, Calif.
- Carter, B., 1982, Neogene displacement on the Garlock fault, California: *Eos Trans. AGU*, 63, 1124.

- Clark, M.M., Grantz, A., and Rubin, M., 1972, Holocene activity of the Coyote Creek fault as recorded in sediments of Lake Cahuilla, in The Borrego Mountain earthquake of April 9, 1968: U.S. Geological Survey Professional Paper 787, p. 112-130.
- Clark, M.M. and LaJoie, K.R., 1974, Holocene behavior of the Garlock fault: Geological Society of America Abstracts with Programs, v 6, 156-157.
- Dawson, T.E., McGill, S.F., and Rockwell, T.K., 2003, Irregular recurrence of paleoearthquakes along the central Garlock Fault near El Paso Peaks, California: Journal of Geophysical Research, B, Solid Earth and Planets, v. 108, no. 7, p. 29.
- Gath, E.M., Gonzalez, T. and Rockwell, T.K., 1992, Slip rate of the Whittier Fault based on 3-D trenching at Brea, southern California (abstract), in *Geological Society of America Cordilleran Section Meeting*, 11-13 May, Eugene, Oregon, Geological Society of America, Cordilleran Section, Anaheim, California, Vol. 24, p. 26.
- Gurrola, L.D., and Rockwell, T.K., 1996, Timing and slip for prehistoric earthquakes on the Superstition Mountain fault, Imperial Valley, southern California: Journal of Geophysical Research, v. 101, no. B3, p. 5977-5985.
- Harris, R.A., and Day, S.M., 1993, Dynamics of fault interaction: Parallel strike-slip faults: Journal of Geophysical Research, v. 98, p. 4461-4472.
- Janecke, S.U., Kirby, S., Langenheim, V., Steely, A.N., Dorsey, R. J., Housen, B., Lutz, A., 2005, High geologic slip rates on the San Jacinto fault zone in the SW Salton Trough, and possible near-surface slip deficit in sedimentary basins; Geological Society of America, 2005 annual meeting, v. 37, no. 7, p 275.
- Kendrick, K.J., Morton, D.M., Wells, S.G., and Simpson, R.W., 2002, Spatial and temporal deformation along the northern San Jacinto fault, southern California; Implications for slip rates; Bulletin of the Seismological Society of America, v.92, no.7, p. 2782-2802.
- Kendrick, K.J., and Fumal, T.E., 2005, Paleoseismicity of the northern San Jacinto fault, Colton and San Bernardino, southern California; Preliminary results: Geological Society of America Abstracts with Programs, v. 37, p. 559
- Magistrale, H., and Rockwell, T., 1996, The central and southern Elsinore fault zone, southern California: Bulletin of the Seismological Society of America, v. 86, p. 1793-1803.
- McGill, S.H.F., 1992, Paleoseismology and neotectonics of the central and eastern Garlock fault, California: Ph.D. dissertation, California Institute of Technology, Pasadena, CA.
- McGill, S.F., and Sieh, K., 1991, Surficial offsets on the central and eastern Garlock fault associated with prehistoric earthquakes: Journal of Geophysical Research, v. 96, no. B13, p. 21597-21621.
- McGill, S., and Sieh, K.E., 1993, Holocene slip rate of the central Garlock fault in southeastern Searles Valley, California: Journal of Geophysical Research, v. 98, no. B8, p. 14217-14231.
- McGill, S.F., 1993, Late Quaternary slip rate of the Owl Lake Fault and maximum age of the latest event on the easternmost Garlock Fault, S. California; Geological Society of America, 89th annual Cordilleran Section meeting and 46th annual Rocky Mountain Section meeting: Abstracts with Programs - Geological Society of America, v. 25, no. 5, p. 118.
- McGill, Sally, 1998, Preliminary slip-rate estimate for the Owl Lake fault, California, in Finding Faults in the Mojave, San Bernardino County Museum Association Quarterly, v. 45, no. 1,2, edited by James P. Calzia and Robert E. Reynolds, pp. 84-87, 1998.

- McGill, S.F., and Rockwell, T., 1998, Ages of late Holocene earthquakes on the central Garlock Fault near El Paso Peaks, California: *Journal of Geophysical Research, B, Solid Earth and Planets*, v. 103, no. 4, p. 7265-7279.
- McGill, S.F., Anderson, H., Daneke, T., Grant, J., Slates, M., Stroud, J., Tegt, S.K., and McGill, J.D., 2003, Slip rate of the western Garlock Fault near Lone Tree Canyon, Mojave Desert, California; Geological Society of America, Cordilleran Section, 99th annual meeting: Abstracts with Programs - Geological Society of America, v. 35, no. 4, p. 64.
- McGill, S.F., Wells, S. G., Kuzma Anderson, H., Fortner, S.K., and McGill, J.D., submitted 2006, Slip rate of the Western Garlock fault, rate of soil development and paleoclimatic implications at Clark Wash, near Lone Tree Canyon, Mojave Desert, California: *GSA Bulletin*
- Mezger, L.L., and Weldon, R.J., 1983, Tectonic implications of the Quaternary history of lower Lytle Creek, southeast San Gabriel Mountains: *Geological Society of America Abstracts with Programs*, v. 15, no. 5, p. 418.
- Millman, D.E. and Rockwell, T.K., 1986, Neotectonics of the Elsinore fault in Temescal Valley, California: in *Guidebook and Volume on Neotectonics and Faulting in Southern California* (P. Ehlig, ed.), Cordilleran Section, Geological Society of America, p.159-166.
- Morton, D.M., Matti, J.C., Miller, F.K., and Repenning, C.A., 1986, Pleistocene conglomerate from the San Timoteo badlands, southern California--Constraints on strike-slip displacements on the San Andreas and San Jacinto faults: *Geological Society of America Abstracts with Programs*, v. 18, no. 2, p. 161
- Nazareth, J.J., and Hauksson, E., 2004, The seismogenic thickness of southern California crust: *Bulletin of the Seismological Society of America*, v. 94; no. 3; p. 940-960; doi:[10.1785/0120020129](https://doi.org/10.1785/0120020129).
- Pinault, C.T. and Rockwell, T.K., 1984, Rates and sense of Holocene faulting on the southern Elsinore fault: further constraints on the distribution of dextral shear between the Pacific and North American Plates: *Geological Society of America Abstracts with Programs*, v. 16, no. 6, p. 624.
- Pollard, W.J., and Rockwell, T.K., 1995, Late Holocene slip rate for the Coyote Creek fault, Imperial County, California: *Geological Society of America Abstracts with Programs*, v. 27, no. 5, p. 72.
- Rasmussen, G.S., 1982, Historic earthquakes along the San Jacinto fault zone, San Jacinto, California: in *Neotectonics in Southern California*, GSA Cordilleran Section 78th Annual Meeting Volume and Guidebook, Field Trip No. 4, 115–121.
- Rockwell, T.K., 1989, Behavior of individual fault segments along the Elsinore-Laguna Salada fault zone, southern California and northern Baja California--Implications for the characteristic earthquake model, in Schwartz, D.P., and Sibson, R.H., eds., *Proceedings of Conference XLV--Fault segmentation and controls of rupture initiation and termination: U.S. Geological Survey Open-File Report 89-315*, p. 288-308.
- Rockwell, T., 1990, Holocene activity of the Elsinore fault in the Coyote Mountains, southern California, in Rockwell, T., ed., *Western Salton trough soils and neotectonics: Friends of the Pleistocene, Field Trip - 1990, Guidebook*, p. 30-42.
- Rockwell, T.K., McElwain, R.S., Millman, D.E., and Lamar, D.L., 1986, Recurrent late Holocene faulting on the Glen Ivy North strand of the Elsinore fault at Glen Ivy marsh, in Ehlig, P.L., ed., *Neotectonics and faulting in southern California: Geological Society of*

- America, 82nd Annual Meeting of the Cordilleran Section, Guidebook and Volume, p. 167-175.
- Rockwell, T.K., and Pinault, C.T., 1986, Holocene slip event on the southern Elsinore fault, Coyote Mountains, southern California, in Ehlig, P.L., ed., Neotectonics and faulting in southern California: Geological Society of America, 82nd Annual Meeting of the Cordilleran Section, Guidebook and Volume, p. 193-196.
- Rockwell, T.K., Klinger, R., and Goodmacher, J., 1990, Determination of slip rates and dating of earthquakes for the San Jacinto and Elsinore fault zones, in Kooser, M.A., and Reynolds, R.E., eds., Geology around the Margins of the eastern San Bernardino Mountains, Volume 1: Inland Geological Society, Redlands, p. 51-56.
- Rockwell, T.K., Gath, E.M., and Gonzalez, T., 1992, Sense and rate of slip on the Whittier fault zone, eastern Los Angeles Basin, California: Proceedings of the Association of Engineering Geologists 35th Annual Meeting, p. 679
- Rockwell, T., Burgmann, M., and Kinney, M., 2000, Holocene slip rate of the Elsinore fault in Temecula Valley, Riverside County, CA *in* Geology and enology of the Temecula Valley: Birnbaum, B.B. and Cato, K., editors, p. 105-118.
- Rockwell, T., Seitz, G., Dawson, T., and Young, J., 2006, (abstract) The long record of San Jacinto fault paleoearthquakes at Hog Lake: Implications for regional patterns of strain release in the southern San Andreas fault system: Seismological Research Letters, v 77, p. 270.
- Sharp, R.V., 1981, Variable rates of late Quaternary strike slip on the San Jacinto fault zone, southern California: Journal of Geophysical Research, v. 86, p. 1754-1762.
- Thorup, K.M., 1997, Paleoseismology of the central Elsinore fault in southern California-- Results from three trench sites: San Diego, California, San Diego State University, unpublished M.S. thesis, 94 p.
- Topozada, T.R., Branum, D.M., Reichle, M.S., and Hallstrom, C.L., 2002, San Andreas fault zone, California: $M \geq 5.5$ earthquake history: Bulletin of the Seismological Society of America, v. 92, no. 7, p. 2555-2601.
- U.S. Geological Survey and California Geological Survey, 2006, Quaternary fault and fold database for the United States, accessed May, 2006, from USGS web site: <http://earthquake.usgs.gov/regional/qfaults/>.
- Vaughan, P.R., Thorup, K., and Rockwell, T.K., 1999, Paleoseismology of the Elsinore fault at Agua Tibia Mountain, southern California: Bulletin of the Seismological Society of America, v. 89, p. 1447-1457.
- Vedugo, D., Ragona, D., and Rockwell, T., 2006, New paleoseismic results from the southern San Jacinto fault zone: 2006 Southern California Earthquake Center Annual Meeting abstract volume, p. 175.
- Weldon, R.J., II, McCalpin, J.P., and Rockwell, T.K., 1996, Paleoseismology of strike-slip tectonic environments; Paleoseismology: International Geophysics Series, v. 62, p. 271-329.
- Wesnousky, S.G., 1986, Earthquakes, Quaternary faults, and seismic hazard in California: Journal of Geophysical Research, 91, p. 12,587-12,631.
- Wesnousky, S.G., Prentice, C.S., and Sieh, K.E., 1991, An offset Holocene stream channel and the rate of slip along the northern reach of the San Jacinto fault zone, San Bernardino Valley, California: Geological Society of America Bulletin, v. 103, p. 700-709.

- Wesnousky, S.G., 2006, Predicting the endpoints of earthquake ruptures: *Nature*, v. 444, doi:[10.1038/nature05275](https://doi.org/10.1038/nature05275).
- Wills, C.J., Weldon II, R.J., and Bryant W. A., 2007, California Fault Parameters for the National Seismic Hazard Maps and Working Group on California Earthquake Probabilities 2007: Working Group on California Earthquake Probabilities Uniform California Earthquake-Rupture Forecast Appendix A, 51 p.
- Working Group on California Earthquake Probabilities (WGCEP), 1995, Seismic hazards in southern California - Probable earthquakes, 1994 to 2024: *Bulletin of the Seismological Society of America*, v. 85, no. 2, p. 379-439.